JOURNAL OF Applied Polymer SCIENCE

Sulphurous additives for polystyrene: Influencing decomposition behavior in the condensed phase

Ulrike Braun,[1] Paul Eisentraut,[1] Sabine Fuchs,[2] Peter Deglmann[2]
[1]BAM Federal Institute for Materials Research and Testing, Unter den Eichen 87, Berlin 12200, Germany
[2]BASF SE, Carl-Bosch-Str. 38, Ludwigshafen 67056, Germany
Correspondence to: Dr. U. Braun (E-mail: ulrike.braun@bam.de)

ABSTRACT: The thermal decomposition behaviour of polystyrene (PS) containing sulphur and phosphorus additives was investigated, using thermogravimetry coupled with Fourier transform infrared spectroscopy (TGA-FTIR). It was found that the additives influence the decomposition process of the polymer in the condensed phase, resulting in a decrease in styrene monomer formation and an increase in styrene oligmer derivatives. Via reference measurements with binary mixtures it was found that the presence of sulphur additives influences the radicalic decomposition process of PS. In combination with quantum chemical calculations it was concluded that this is due to the formation of radicals that abstract hydrogen from the polymer matrix at lower temperatures, disfavouring the radicalic decomposition pathway leading to styrene. © 2014 Wiley Periodicals, Inc. J. Appl. Polym. Sci. **2015**, *132*, 41665.

KEYWORDS: degradation; theory and modeling; thermogravimetric analysis; polystyrene

Received 21 July 2014; accepted 21 October 2014
DOI: 10.1002/app.41665

INTRODUCTION

It is documented in the literature that a mixture of elemental sulphur and phosphorus compounds, e.g., aryl phosphates, imparts flame retardancy to polystyrene (PS) materials.[1,2] Recent research has shown that organic sulphur compounds, too, can play a synergistic role similar to that of elemental sulphur.[3,4] Although the mechanism of phosphorous compounds as flame retardants is most probably flame poisoning (PS, independent of its additivation, burns without leaving residue), the synergistic mode of action of sulphur compounds, and their interaction with the polymer matrix and/or PS decomposition intermediates, are much less clear. Therefore, the scope of this work is the analysis of the thermal decomposition of these PS materials containing sulphur and/or phosphorus compared with the pure polymer. A special focus here is the influence of the additives on the polymer degradation process in the condensed phase.

The thermal decomposition of PS takes place through radical processes.[5–8] It is well known that most of the volatiles are evolved from chain-end initiation and not from random scission. By means of a hypothetical backbone scission of the homolytic bond, first a secondary radical is formed, which depolymerises further to styrene monomers; and second, a primary radical is formed, which reacts via hydrogen transfer to oligomeric species (such as dimers, trimers, alpha methyl styrene) before also depolymerizing as secondary radicals. It is not fully clear to what extent small amounts of head-to-head linkages, yielding two secondary radicals upon cleavage, contribute to or even dominate the generation of homolytic radicals. Alternatively, the decomposition of still intact PS chains can be initiated by radicalic hydrogen abstraction from the polymer backbone, resulting in the formation of tertiary radicals, which decay into olefin-terminated macromolecules and—again—active radicals from secondary depolymerization. Furthermore, disproportionation or various radical recombination reactions will occur, slowing down the decomposition of PS.

It is possible to influence the thermal degradation profile in the condensed phase by cross-linking the aromatic side groups of PS using diols as alkylating agents and zeolites as catalysts,[9,10] by adding divinyl derivatives,[11] or by irradiating samples of the material with gamma sources.[12] Further studies were performed using catalysts for polymer backbone cleavage with the aim of recycling or fuel production,[13–15] or via the addition of nanoclay, which slows down the volatile release by barrier formation, thus influencing the radical transfer reaction during pyrolysis with the intention to obtain a flame-retarding effect.[16,17]

Phosphorus-based additives do not influence the PS pyrolysis mechanism.[18–22] In fire, however, when phosphorus compounds are released in the gas phase, they suppress the oxidation process of fuel, resulting in incomplete oxidation (instead of the rather exothermic formation of CO_2 and water), and thus an increase in partly oxidized decomposition products (formation of CO and smoke). This process will not affect the pyrolysis

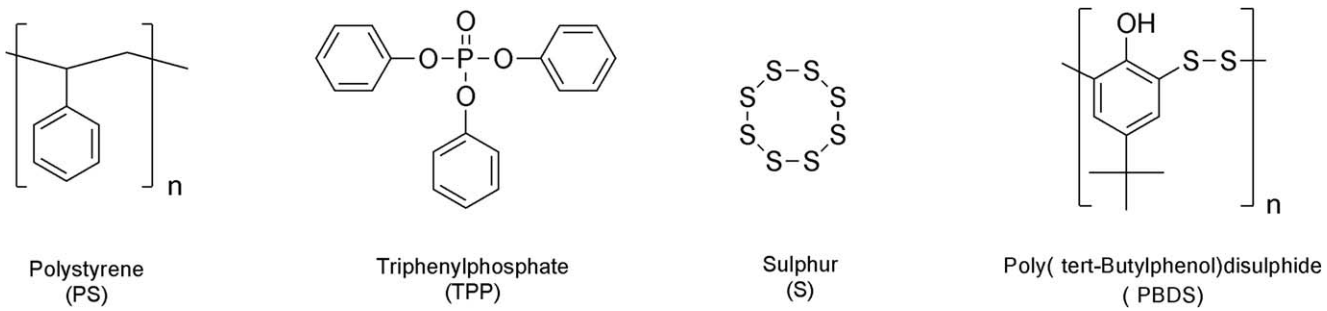

Figure 1. Chemical structure of the additives.

profile or PS residue formation. When phosphorus remains in the residue it can form a barrier. This barrier may slow down the pyrolysis gas release rate and, in so doing, influence the chemistry of radicals during pyrolysis. In contrast, no active influence of phosphorus on the PS scission is found.

For additives containing bromine, an influence on the PS pyrolysis profile was observed in the solid phase, although the fire retardant effect always discussed is the flame inhibition in the gas phase.[23] A clear interaction in the solid phase was observed for brominated flame retardants and antimony trioxide with PS.[24] According to the authors, the additives reduce the thermal stability of PS and decrease the formation rate of monomers. It was proposed that the additives abstract hydrogen from the polymer backbone, thus accelerating the formation of styrene monomers. The thermodynamics of PS degradation was discussed using molecular modelling.[1] In the solid phase, possible radical interactions by bromine derivatives, but also by elemental sulphur und phosphorous additives, were presented in another work, where the altered decomposition mechanism is explained by a process of hydrogen abstraction from the polymer backbone and subsequent double bond formation.

In this study, elemental sulphur (S) and an alternative to elemental sulphur were used. The alternative sulphur compound is a polymeric disulphide, a substituted, sterically hindered phenol, poly(*tert*-butylphenol)disulphide (PBDS). Its current use is as a vulcanization agent for rubber. As the phosphorus compound, triphenyl phosphate (TPP) was used. TPP is well known as flame retardant in polycarbonate materials.[25]

The degradation behavior was analyzed using thermal decomposition experiments with evolved gas analysis. Various concentrations of the additives in the PS matrix were analyzed. Furthermore, a stoichiometrically mixed, binary composition of the single additives was prepared and analyzed to focus on the interaction of the additives. The results were discussed in the context of the common PS decomposition models from the literature. It is not the aim of this work to assess the activity of phosphorus in the gas phase, nor its activity as a flame retardant. We focus on the influence of the additives on the decomposition behavior of PS.

Table I. Composition of the Investigated Materials

Parts per hundred parts PS	TPP	S-Source
PS	0	0
PS-TPP	5	0
PS-S	0	2.5
PS-PBDS	0	5
PS-TPP-S	5	2.5
PS-TPP-PBDS	5	5
PS-TPP(2.5)-PBDS(5)	2.5	5
PS-TPP(5)-PBDS(2.5)	5	2.5

EXPERIMENTAL

Materials

The molecular structures of the individual organic compounds are shown in Figure 1. Polystyrene PS 158 K with an MVR (200°C, 5 kg) of 3 mL/10 min and a Vicat-softening temperature (VST/A/50) of 106°C (Styrolution GmbH) was melted and mixed with the additives in the amounts given in Table I in a midi extruder (DSM, Gelen). The extrusion temperature was 180°C, and the polymer melt was extruded over a period of 10 min. The amounts of additives, i.e., sulphur (Sigma-Aldrich), triphenylphosphate (TPP, Sigma-Aldrich) and PBDS (MLPC/Arkema) given in Table I are parts per hundred (phr) calculated on the basis of 100 parts of polymer (PS).

The cooled polymer melt was released from the extruder and subsequently cut into small pieces. These were then dissolved in dichloromethane (Sigma-Aldrich), poured into small vessels, and stored at room temperature for 48 h to slowly evaporate the solvent. The polymer samples were transformed into foamed foils by rapidly evaporating the residual solvent at 110°C over a period of 30 min. The densities of the foamed foils obtained in this procedure were between 10 and 60 g/l. The exact composition of the investigated materials is summarised in Table I.

The analysis of the dispersion into specific TPP signals by FTIR imaging reveals a homogeneous distribution. The addition of the additives results in a slight temperature shift towards a lower glass transition temperature in accordance with the increased plasticizing additive concentration in the polymeric material (DSC measurements).

Methods

Thermal decomposition of the materials was investigated by means of thermogravimetric analysis (TGA) (TGA/SDTA 851, Mettler Toledo). Measurements were performed under nitrogen with a gas flow rate of 30 mL min^{-1}. Sample masses were 10 mg. TGA was coupled with a Fourier transform infrared spectrometer (FTIR) (Nexus 470, Nicolet Instruments) to identify the evolved

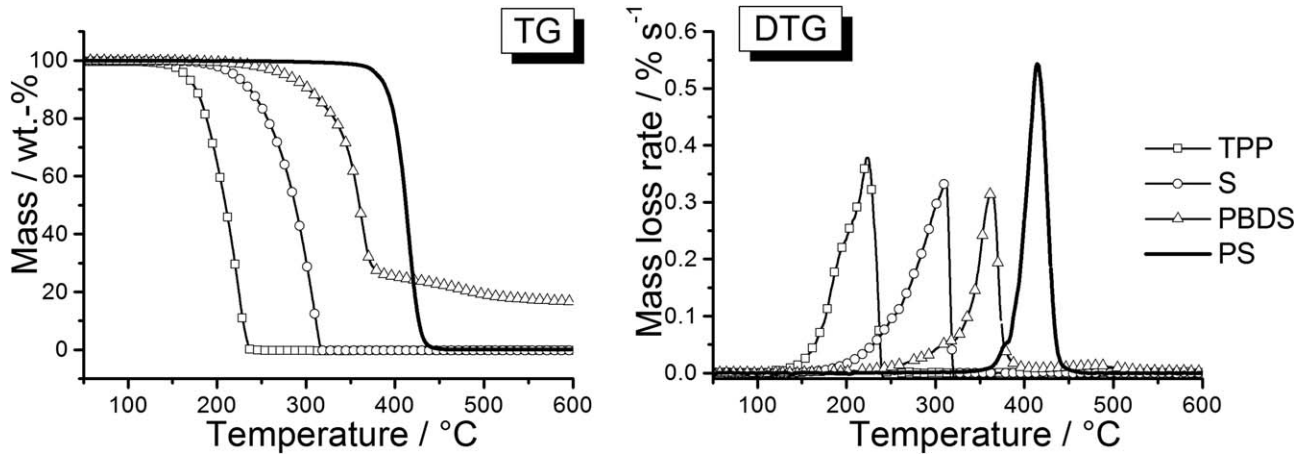

Figure 2. TGA results of single materials.

decomposition products. The temperature of the transfer line from TGA to FTIR was 250°C, and the temperature of the gas cell was 260°C. Product release rates of evolved decomposition products were determined using the peak height of characteristic vibrations in the IR spectrum. For reproducible test results at least two to three measurements were taken for each specimen. The wave numbers in the text are accurate to ±4 cm^{-1}.

The FTIR investigations of solids were performed using attenuated total reflection (ATR, Smart Orbit Accessory) in a Nicolet 6700 FTIR spectrometer (Thermo Scientific) with a DTGS KBr detector. To obtain a spectrum, 32 scans were taken at an optical resolution of 4 cm^{-1}. For the ATR-FTIR investigations the materials were pressed on the diamond cell to achieve surface-sensitive test results. For reproducible test results at least two to three measurements were taken for each specimen. The wave numbers in the text are accurate to ± 4 cm^{-1}.

Computational Details

In the quantum chemical study, Gibbs free energies G were calculated for a temperature of 300°C, as this thermodynamic function is directly associated with chemical equilibrium. All species were assumed to be generated initially in the condensed phase, which should be a valid assumption for all reactions considered, although any volatile product will, of course, evaporate as soon as it reaches the surface of the molten decomposing PS matrix. The PS models considered were chosen to be fully syndiotactic; changes in results occurring upon transition to isotactic or stereo-irregular materials (which technical PS grades typically are) were not considered for the sake of simplicity.

Molecular structures were optimized with the Becke-Perdew-86 functional[26–28] (BP86) level of theory using an SV(P)[29] basis set in combination with the assumption of an electric conductor (dielectric constant $\varepsilon = \infty$) according to the COSMO solvation model.[30] For a more accurate description of the actual chemical reaction in the gas phase, as a DFT method the M06 functional[31] was chosen in combination with a def2-TZVP basis set[32] (using the same valence basis functions as within TZVP; but with polarization functions from Dunning's cc-pVTZ basis set). Thermodynamic functions, omitting the vibrational partition function, were evaluated for a temperature of 300°C according to standard statistic thermodynamic expressions. A solvation treatment was performed using the COSMO-RS method,[33] as has been described elsewhere for application to radical polymerization.[34] This requires further calculations at the BP86 level with a def-TZVP[35] basis set, assuming both a gas and an electric conductor environment. A PS-octamer was chosen as the "solvent." All calculations at the BP86 level of theory

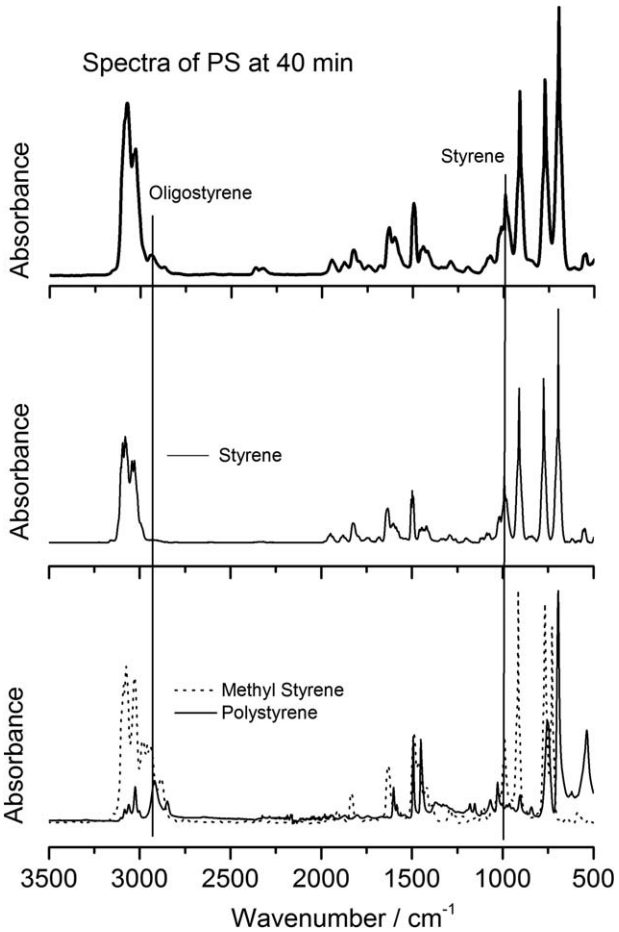

Figure 3. Exemplary FTIR spectra of evolved gas analysis from PS at DTG_{max} (top) with reference spectra from database (below).

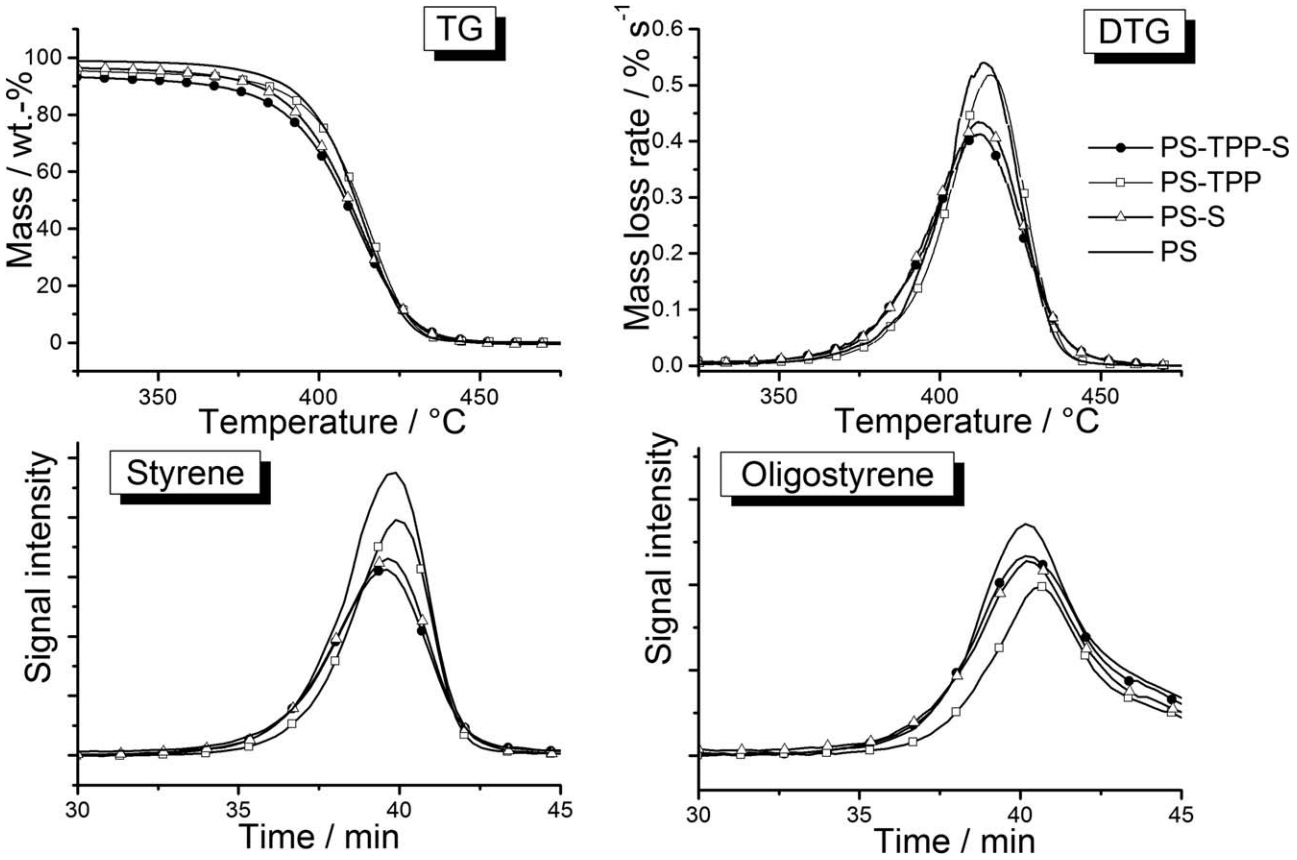

Figure 4. TGA-FTIR results of PS materials; top: TGA and DTG data, bottom: release rates of characteristic decomposition products.

were performed with the program package TURBOMOLE.[36] Single-point energies at the M06 level were computed with the program package NWChem.[37]

An empirical entropic correction of -80 J mol^{-1} K^{-1} (obtained by checking which correction leads to $\Delta G = 0$ at 350°C for PS decomposition to styrene) was applied to all processes leading to bond cleavage. Furthermore, for the H-abstraction transition states in Figure 13, unrealistically negative activation entropies would be obtained by the above-mentioned treatment, e.g., as contributions to the vibrational partition function (typically making the activation entropy less negative) can not be included in the large models considered here (low-frequency modes). For the smaller but rather realistic model Ph-S· + Ph-CH_3 → Ph-SH + Ph-CH_2, the total activation entropy including the vibrational partition function was computed to be -90 J mol^{-1} K^{-1} (average between forward and backward reaction). It was found that, for the larger models, around the same value is obtained when activation entropies were shifted by $+130$ J mol^{-1} K^{-1}, which was done to obtain the results of Figure 13.

RESULTS AND DISCUSSION

Decomposition of the Single Components

The single materials can be characterized via their characteristic signals detected with ATR-FTIR. PS shows characteristic signals of aromatics at 3057, 3026, 757, 695, and 542 cm^{-1} as well as aliphatics at 2924, 2852, 1493, and 1452 cm^{-1}. TPP can be identified by unambiguous bands at 1297, 1194, 1163, 1010, and 959 cm^{-1}. Specific PBDS signals are the phenolic signals at 3400, 1582, 1475, 1445, 820, and 720 cm^{-1} as well as the *tert*-butyl group at 2955, 2900, and 2865 cm^{-1}.

The decomposition behavior of the single components in TGA is shown in Figure 2. According to the TGA analysis of the single components, it is expected that most of all the materials pyrolyse in different temperature regions.

The decomposition temperature of PS is clearly higher than that of TPP, S and of PBDS. Decomposition of PS starts at 350°C and the maximum of the DTG signal is observed at 415°C. As gaseous decomposition products only styrene monomer is observed along with small fragments of the polymer chain, such as styrene dimers and trimers as well as derivatives of styrene like alpha methyl styrene. No residue remains. As an example, a decomposition product spectrum of PS is shown in Figure 3 with reference spectra. The results observed are in accordance with the literature.[5–8] The vertical lines in the figure represent the chosen signals for product release rates (signal integration versus time): for styrene the band high at 989 cm^{-1} was chosen, for oligostyrene the band high at 2940 cm^{-1}.

The mass loss of TPP starts at 160°C and reaches the maximum DTG signal at 220°C. In evolved gas analysis it can be observed that the obvious mass loss is dominated by vaporization of the

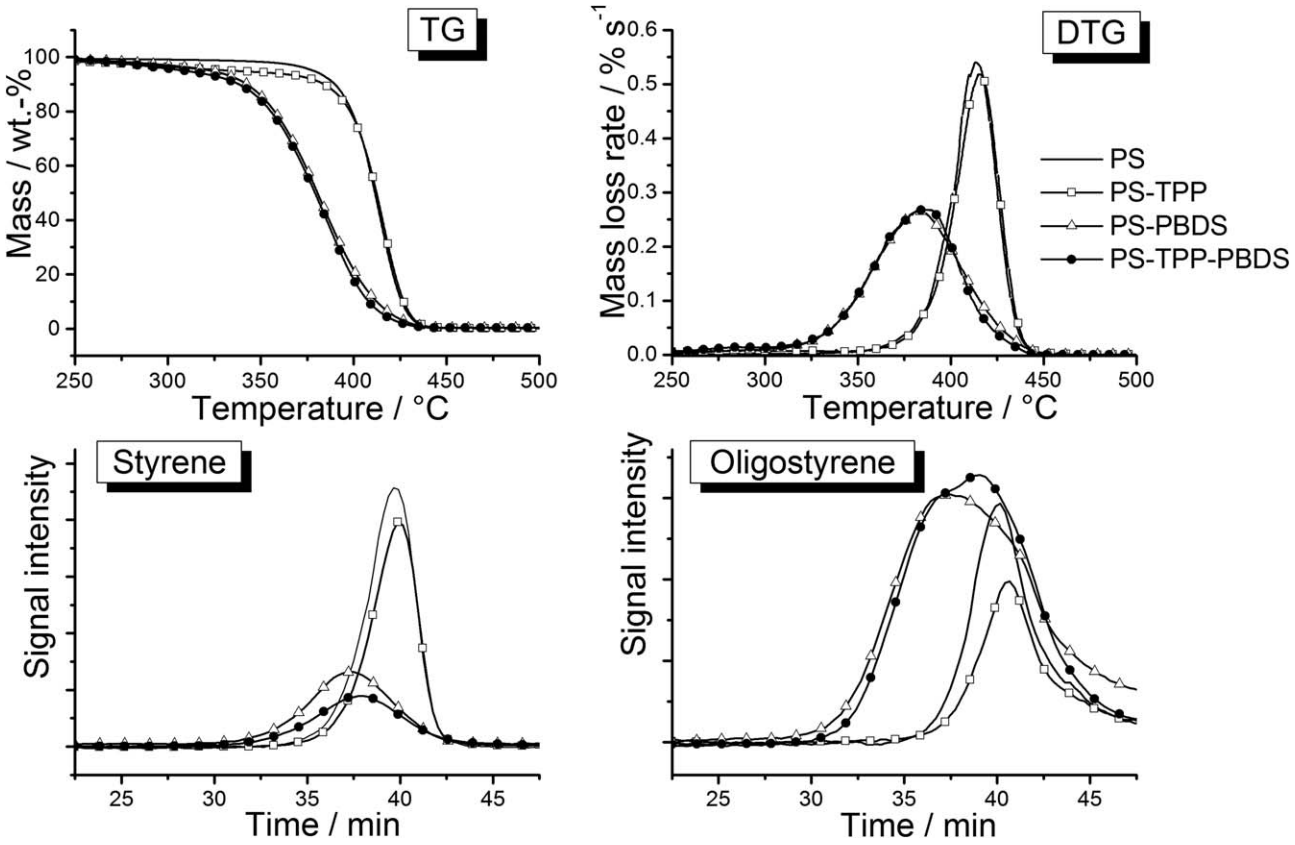

Figure 5. TGA-FTIR results of PS materials; top: TGA/DTG data, bottom: release rates of characteristic decomposition products.

complete molecule. No residue remains. The vaporization of TPP under these conditions is also documented in the literature.[25]

Sulphur begins losing mass at around 185°C and reaches a maximum at 310°C. Above 320°C, no more residue can be detected. The shape of the DTG signals indicates vaporization of the component. Due to the infrared inactivity of S_8 and all other potential pyrolysis products, no speciation of gaseous decomposition products is possible.

PBDS degradation consists of two steps: Decomposition starts at 220°C and maxima in DTG signal are observed at 350 and 480°C. The first, major decomposition step amounts to about 75 wt %, whereas the second, minor step involves only 10 wt % mass loss. A residue of 15 wt % remains under nitrogen flow. For PBDS various decomposition products are observed in gaseous decomposition analysis during the first, major decomposition step. There are derivatives containing an intact phenol ring, such as *tert*-butyl-phenol and a number of small decomposition products containing sulphur such as carbon disulphide, carbonyl sulphide and sulphur dioxide. In addition, the release of carbon dioxide and water was observed. During the second, minor step only methane is released, indicating anaerobic char decomposition. Maybe also some carbon components containing sulphur remain in the residue.

Decomposition Behavior of the Polymeric Materials

To separate the effects of the single additives, PS, PS-TPP, the PS-sulphur component and the PS-TPP-sulphur component were compared systematically by means of TGA-FTIR measurements.

The results for the combination of PS-TPP-S are shown in Figure 4. In the TGA data, no significant change of the decomposition behavior of PS was observed; all material decomposes in a single step, without the formation of any residue. For PS-TPP, the major start of mass loss, the maximum of the DTG signal and the residue formation are no different from those of pure PS. In the decomposition product release, too, no significant difference was observed for the release of styrene and oligomeric styrene derivatives. However, a slight but reproducible effect can be observed when S is added. Materials containing S show a slightly reduced onset temperature and a reduction in the DTG signal. Evolved gas release spectra also show no significant difference from the decomposition product spectra—only styrene and oligostyrene can be detected. To evaluate product release rates, characteristic signals are chosen for the single components; these are marked in Figure 3 by straight lines. No separation between styrene dimers and trimers or methyl styrene is possible, therefore only the sum of oligostyrene is used. TPP itself was not observed as a volatile decomposition product because it condenses in the transfer line. With respect to the observed product release rates, no systematic differences between the materials can be observed, although the different additive content in the various materials was considered.

In the combinations of PS-TPP-PBDS, the situation is different (Figure 5). Adding PBDS to PS significantly influences pyrolysis

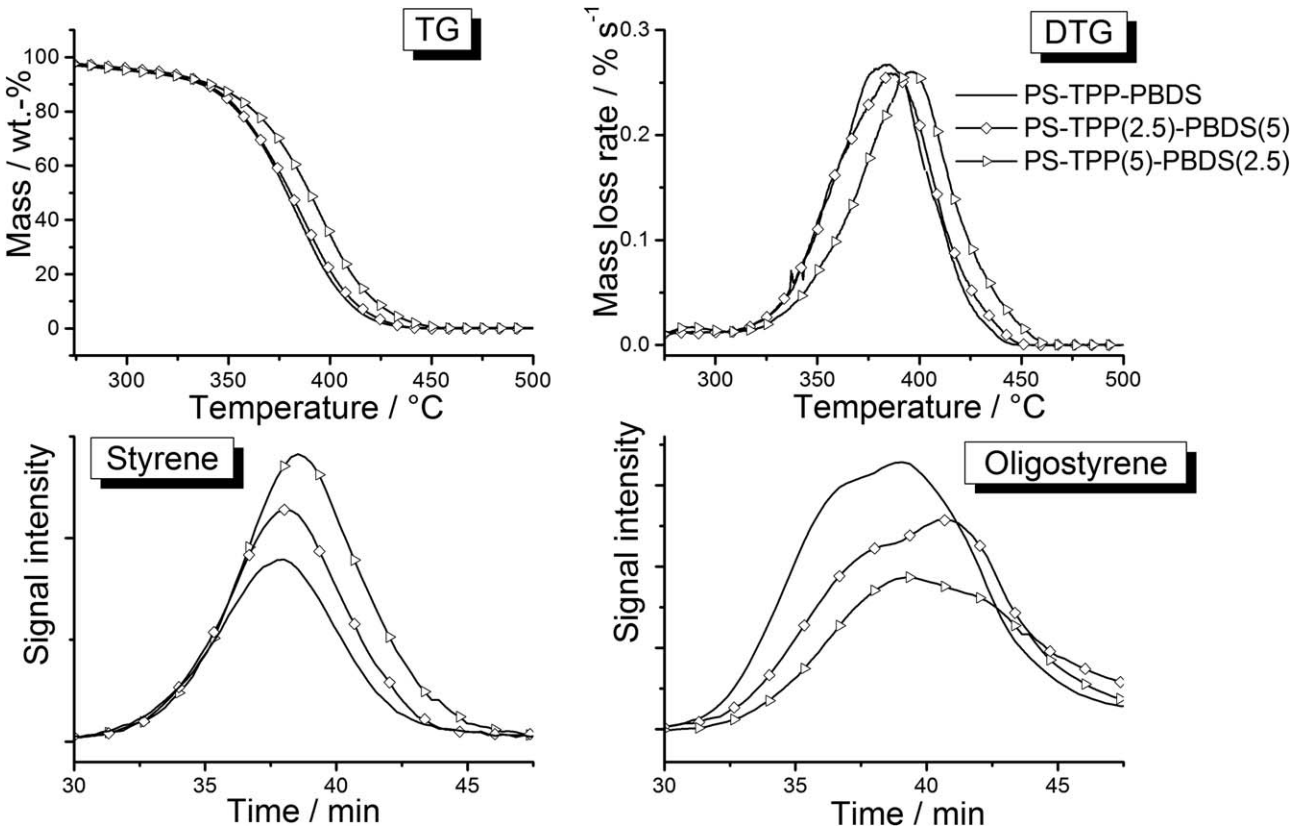

Figure 6. TGA-FTIR results of PS materials; top: TGA/DTG data, bottom: release rates of characteristic decomposition products.

behavior. Decomposition starts significantly earlier, and the maximum of the DTG peak is observed at 385°C. No residue remains, although it should be mentioned that the expected residue for the PBDS content derived from the DTG of the pure additive is on the scale of the error of the measurements of those small quantities of PBDS applied in the PS matrix. Besides the dramatic change in the decomposition temperature range of the PS matrix due to the presence of PBDS, the ratio of observed decomposition products is changed as well. The formation of styrene monomer is reduced, and the release of oligomeric styrene derivatives is increased, which is most probably a consequence of the earlier decomposition and thus a lower preference for the styrene produced in the low molecular decomposition.

From these results it is clear that the decomposition of the PS matrix is influenced more strongly by the sulphur component than by the phosphorus component. To verify this finding, the relative content of sulphur and phosphorus was varied. In the variation of TPP to S content in PS, no significant difference is observed (data not shown). As demonstrated by TGA, neither

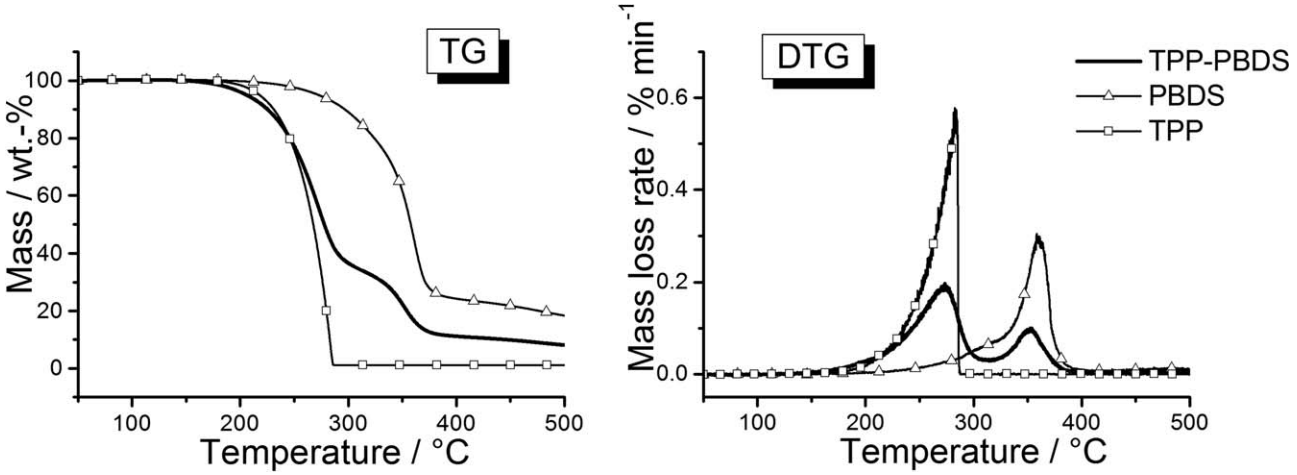

Figure 7. TGA results of binary mixtures.

Table II. TGA Step Size Evaluation of Binary Mixtures (ML = Mass Loss)

	TPP	PBDS	TPP + PBDS
Temp. range RT-315°C			
Exp. ML/wt %	98.7	15.5	65.9
Calc. ML/wt %			57.1
Temp. range 315-385°C			
Exp. ML/wt %		59.2	22.8
Calc. ML/wt %			29.6
Temp. range 385-600°C			
Exp. ML/wt %		9.7	4.2
Calc. ML/wt %			4.9
Residue at 600°C			
Exp. residue/wt %	1.2	15.8	7.3
Calc. residue/wt %			8,5

the decomposition profile nor the evolved gas analysis indicates any difference.

However, the variation in the ratio of TPP to PBDS content in PS-TPP(5)-PBDS(2.5), PS-TPP(5)-PBDS(5) and PS-TPP(2.5)-PBDS(5) shows surprising behavior (Figure 6). First, the peak of the DTG signal of PS-TPP(2.5)-PBDS(5) and PS-TPP(5)-PBDS(5) is shifted to a lower temperatures than for PS-TPP(5)-PBDS(2.5). This means that the temperature of the maximum DTG signal depends on the absolute PBDS content. The increased formation of styrene oligomer species and the decrease in styrene behave as PS-TPP-PBDS > PS-TPP(2.5)-PBDS(5) > PS-TPP(5)-PBDS(2.5). This means that not only the absolute PBDS content influences the product formation rate, but also the relative content of TPP. This indicates a stoichiometric interaction of PBDS and TPP, resulting in a decrease in styrene monomer and increase in oligostyrene formation.

Decomposition Behavior of a Binary Mixture of TPP and PBDS

To analyse this interaction of TPP and PBDS, we mixed the components in a relative mass ratio of 1 : 1 and measured thermal decomposition. Adding TPP to PBDS in such a binary mixture yielded some surprising observations. The raw powder of both additives became liquid after a few minutes and retained this consistence. This observation could be caused by a simple plasticizing effect, but analysis of the "reaction" at room temperature on the FTIR crystal reveals a physico-chemical interaction as well. The characteristic P═O vibration band at 1293 cm^{-1} of TPP and the characteristic broad O─H band of PBDS at 3354 cm^{-1} decrease over time. These transformations indicate the formation of a hydrogen bond between the phenolic hydroxyl group of PBDS and the double-bonded oxygen of the TPP. The decomposition behavior of the binary mixture was analyzed in a TGA experiment, and compared with the decomposition behavior of the single components.

In first approximation the curves of the TGA investigation of this mixture indicate no interaction (Figure 7); however, the detailed step-size evaluation yields an important result (Table II). The first major decomposition step of PBDS-TPP mixture up to 320°C decomposition should be dominated by complete TPP vaporization. But at around 9 wt % this step size is larger than expected. The second decomposition step of the mixture at between 315 and 385°C is about 7 wt % smaller than expected. The high temperature degradation above 385°C and the residue formation correspond to the expected values. In evolved gas analysis no variations could be observed when compared with the decomposition of the single components.

According to the molar mass of the "PBDS monomer" (212 g mol^{-1}) and of TPP (362 g mol^{-1}), the weight mixture of 1 : 1 in the binary mixture corresponds to a stoichiometry of 3 : 2 results. Under the assumption that a stoichiometric interaction takes place, only 2/3 of PBDS interacts with TPP. Considering a complete interaction, the derivation between the measurement and calculated mass loss value of the PBDS-TPP mixture below 320°C would increase to 15 wt % instead of 8.8 wt %. 15 wt % of the initial 50 wt % of PBDS in the binary mixture can be attributed to the component of a molar weight around 63 g. This molecular weight fits very well to a disulphide molecule. We concluded that in binary mixtures TPP accelerates the formation of disulphides from PBDS. This reaction probably occurs through formation of a hydrogen bridge bond between the phenolic hydrogen and the oxygen in TPP (Figure 8). The hydrogen bridge in PBDS could be observed by FTIR measurements during the preparation of mixture, and is common for the thermal behavior of phenolic additives as antioxidants.[38]

Decomposition Pathway of Disulphide in PS

The formation of radicalic sulphur species in the temperature range from 200 to 300°C must influence the decomposition of PS and the formation of gaseous decomposition products from

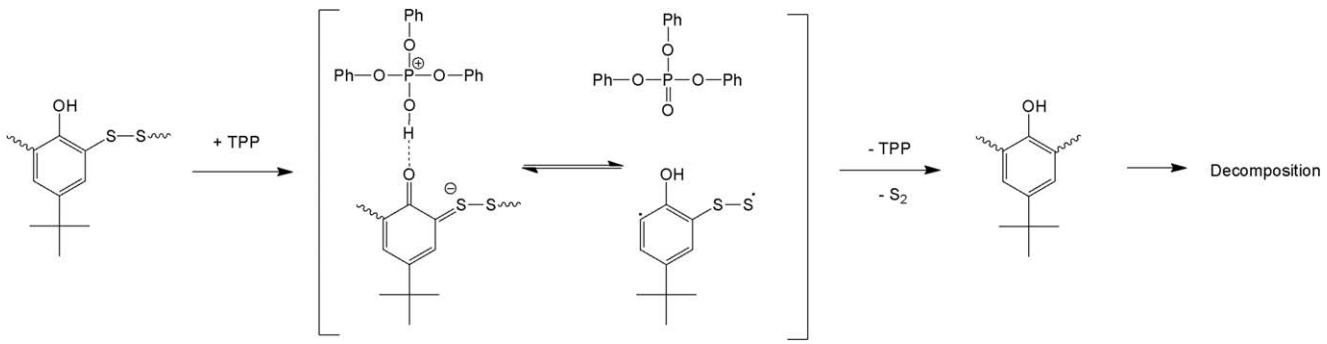

Figure 8. Proposed interaction between TPP and PBDS below 320°C.

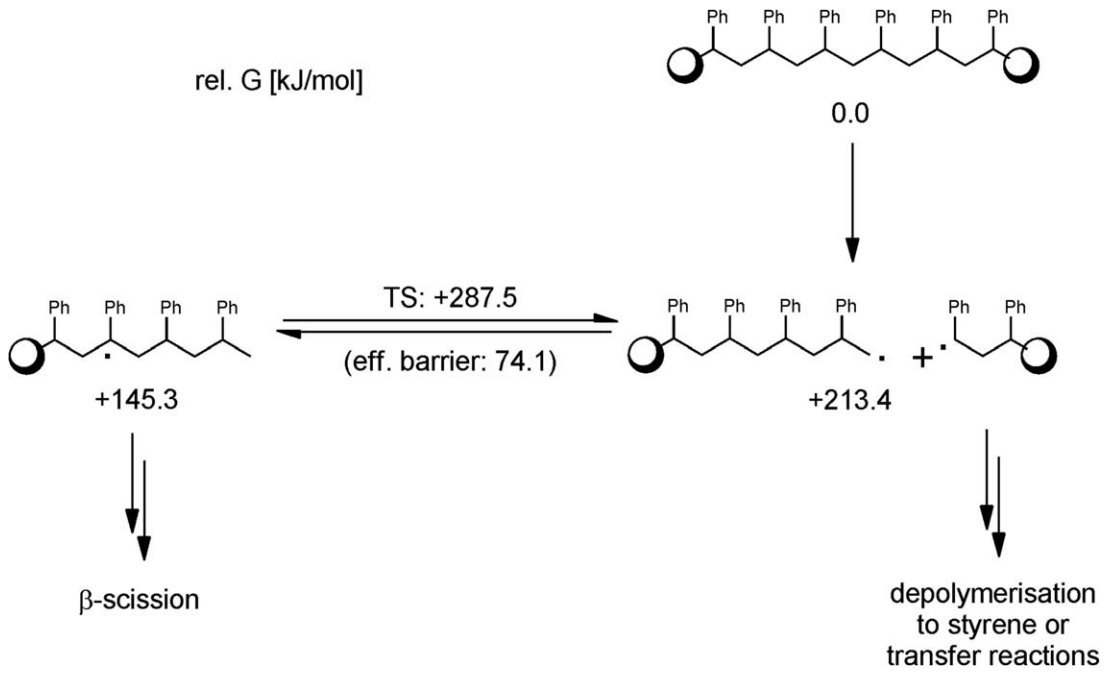

Figure 9. Computed relative Gibbs free energies of radical generation via mid-chain cleavage of PS.

the matrix significantly. The decomposition of PS is shifted to lower temperatures, the formation of styrene monomer is decreased and the formation of oligostyrene is increased. In this temperature range, PS is still in the condensed phase. The presence of TPP shifts the formation of radical sulphur species in PS matrix to lower temperatures, as it was observed in the comparison of various sulphur/phosphorus ratios (see Figure 6).

In the literature it could be found that nascent disulphide components are able to react with multiple bonds. However, the resulting poly(styrene disulphide)[39] is thermally instable and will decompose at temperatures above 200°C in styrene and sulphur species. According to the condensed phase, interactions of additives and PS matrix discussed in the literature,[1,24] we also conclude that the sulphur radicals formed in the solid phase perform the hydrogen abstraction from the polymer backbone and influence the number (and speciation) of radicals during degradation of the PS matrix.

Quantum Chemical Study of the Interactions Between PS and PBDS

To better understand the observed interaction between the PS matrix and the disulphide as well as the origin of the shift in volatile decomposition products at a molecular level, quantum chemical calculations on these issues were also performed.

General Remarks. In the following schemes, relative Gibbs free energies G (for a temperature of 300°C) are given with respect to a reference species (which has typically been chosen to be the starting point of a decomposition reaction). ΔG for any reaction

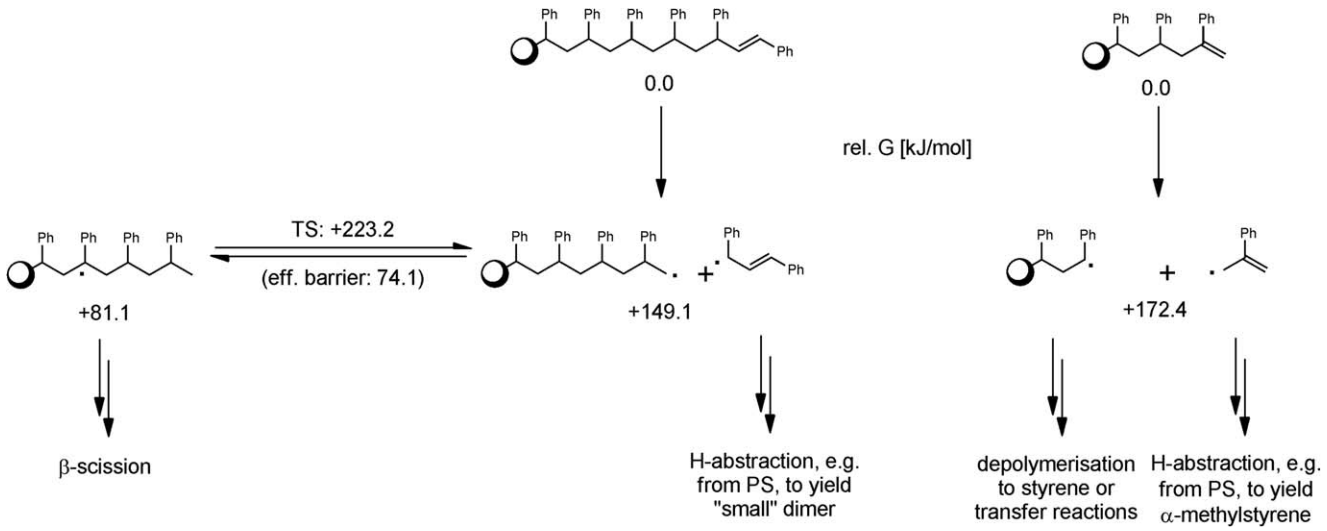

Figure 10. Computed relative Gibbs free energies of radical generation via unsaturated chain-end cleavage of PS.

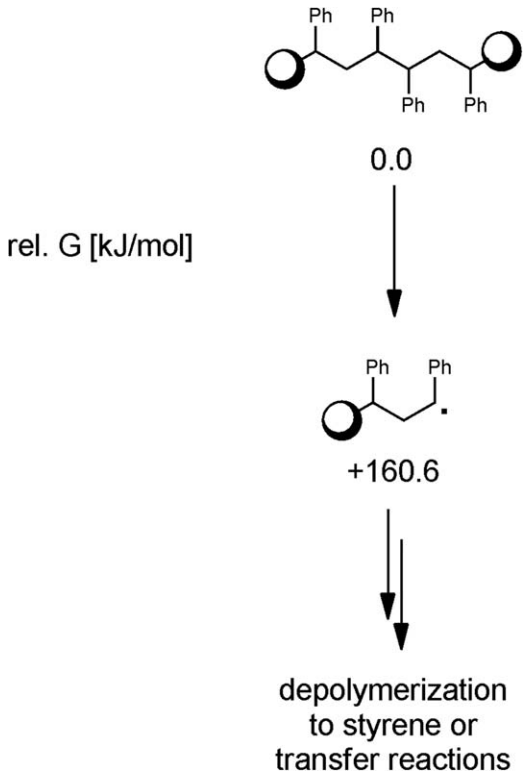

Figure 11. Computed relative Gibbs free energies of radical generation via decomposition of head-to-head linkages of PS.

leading from one species to another in the schemes can be calculated by subtracting the relative G-value of reactant(s) from that of the product(s). Negative ΔG (=exergonic reactions) mean that the products are favored in equilibrium, whereas positive ΔG (=endergonic reactions) indicate that the equilibrium is on the reactant side. However, even intermediates with higher relative G than the reactants can be part of relevant decomposition pathways, as the endergonic intermediates can further react to final products with negative relative G (i.e., an overall negative ΔG). This is the case when products are released into a diluted gas phase and/or transported away from a decomposing material. However, to realize concentrations of species in chemical equilibrium, reaction rates must be sufficiently high. Chemical kinetics of reactions that exhibit an activation barrier depend on Gibbs free energies of activation G^+, which are computed by subtracting the relative G of reactants from that of the corresponding transition state (denoted in the following as TS); for conversions that typically exhibit only small energetic barriers in excess of the reaction thermodynamics (e.g., homolytic bond cleavage), no transition states have been computed.

Radical Generation Within the PS Matrix. Radical decomposition of a pure PS matrix will occur through homolytic cleavage of backbone C—C bonds. The least favorable such event would be a mid-chain cleavage in the absence of any radical-stabilizing groups other than the phenyl substituent (which can provide this stabilization to only one of the generated radicals, of course), for which results are given in Figure 9.

Once this hypothetical, highly endergonic homolysis takes place, it is expected that the primary radical will immediately rearrange to a tertiary radical via H-abstraction, as has been studied here for the most probably preferred intramolecular case. The 1,6-H-shift here exhibits the lowest barrier of 74.1 kJ mol^{-1}, which translates to a rate of 2.1 $\times \cdot 10^{+6}$ s^{-1}. Another such "primary radical backbiting," the 1,4-H-shift, requires a very similar barrier of 75.0 kJ mol^{-1} to be overcome and is thus possible as well. Secondary radical depolymerization and other β-scissions, subsequent chemistries of the products from Figure 9, are considered a few sections below.

As mentioned before, it has been observed that radical PS decomposition takes place preferentially from chain ends. For unsaturated chain ends, formed, e.g., by transfer or β-scission reactions upon polymer synthesis or previous degradation events, much lower Gibbs free energies of homolytic cleavage are computed, as shown in Figure 10.

There are two ways unsaturated chain ends can appear: the disubstituted olefin carrying the polymer and one phenyl group as substituents at different C-atoms (the reference species of the left part of Figure 10) would typically result from transfer reactions during polymerization, whereas a vinylidene terminus (right part of Figure 10) is more likely the result of a previous β-scission. Modeling reveals that the former chain ends represent particularly preferred points of breakage, but vinylidene terminated PS, too, should undergo C—C cleavage at these sites much more easily than the backbone itself (with a difference in Gibbs free energies of still more than 40 kJ mol^{-1}, meaning that the equilibrium constants differ by a factor of more than 10^{+4}). Homolysis is much easier at the unsaturated chain ends because of the very stable allyl radical products, in particular 1,3-diphenyl allyl; formation of the latter more than compensates for even the formation of a primary radical, which should undergo fast stabilization as already discussed above.

Head-to-head linkages would represent another possibility for such preferred points of breakage, as given in Figure 11. Here, too, decomposition will occur much more easily than mid-chain cleavage due to reduced steric repulsion and the fact that two benzylically stabilized radicals are formed. However, as the number of head-to-head linkages is typically very small to even negligible, the contribution of this mechanism to initial radical generation is difficult to predict.

Altogether, from the computations it can be concluded so far that radical formation out of the PS matrix itself will be associated with endergonic reactions that exhibit a ΔG of around +150 to +170 kJ mol^{-1}.

Radical Decomposition of PBDS. Also PBDS decomposition scenarios were also investigated by means of calculations, see Figure 12. First, a homolytic cleavage of the S-S bond as the weakest link in the polymer is the obvious for radicals to form. With a ΔG of less than +80 kJ mol^{-1} at the reaction conditions considered, this definitely represents a possible pathway to aryl monothiyl radicals. However, for decomposition of phenolic structures, reaction out of the keto form can also play a role. Although the loss of aromaticity in the keto tautomer is significantly endergonic by >60 kJ/mol, this tautomerism is predicted to enable another product channel, leading to phenoxy radicals

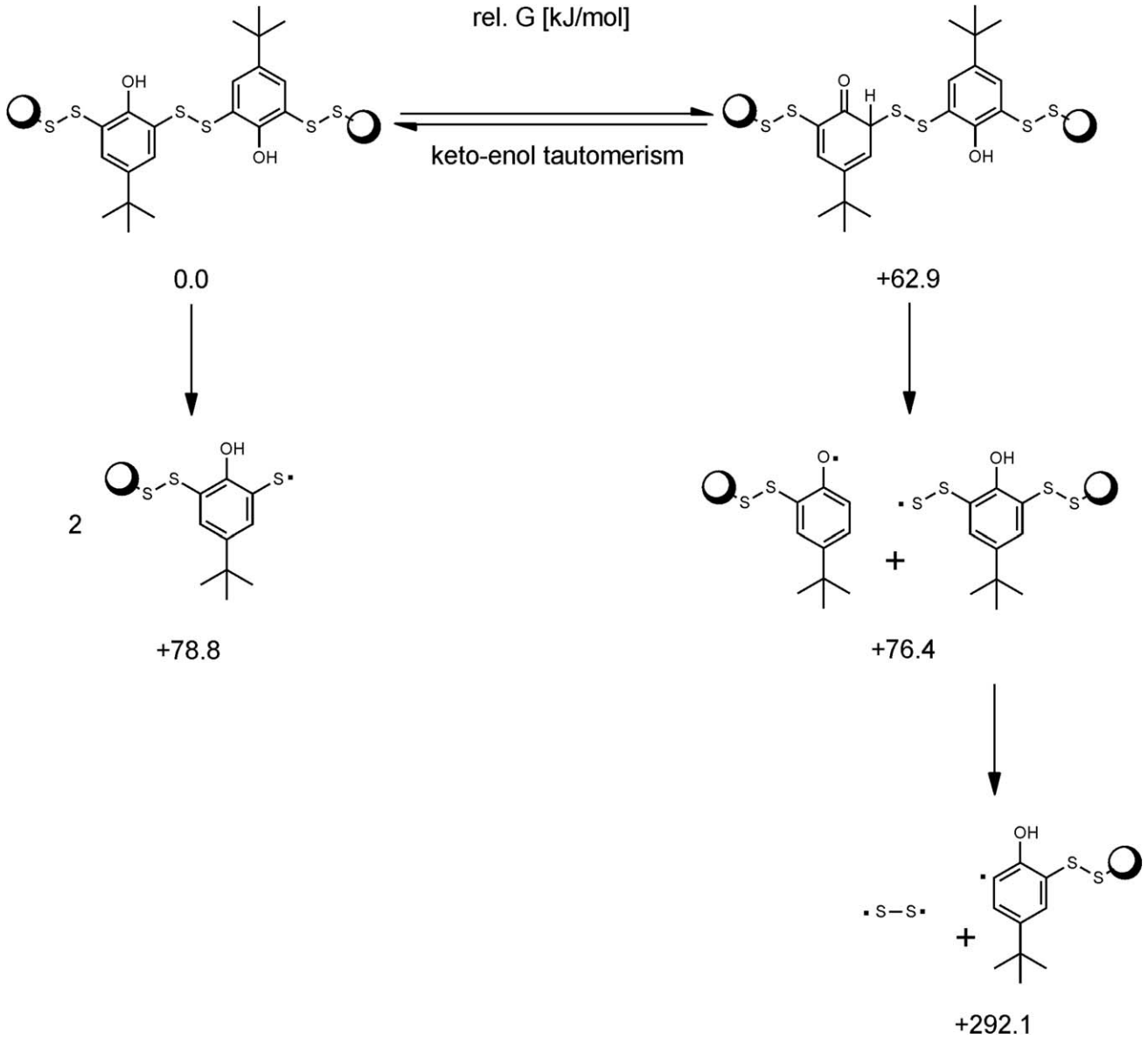

Figure 12. Computed relative Gibbs free energies of PBDS decomposition.

and aryl dithiyl radicals—both of these decomposition pathways are associated with very similar ΔG. For the latter dithiyl radicals, a further decay to S_2 and aryl radicals is possible in principle, but rather prohibitive from a thermodynamic point of view; however, larger sulphur chains could be generated via cascades of radical group transfer reactions involving attack of dithiyl radicals at intact disulphide groups.

From this, it can be expected that in the case of PBDS pyrolysis, singly or even not S-substituted phenols are formed as well as sulphur; of course, it can also not be fully excluded that the observed phenols are leftovers from PBDS synthesis. In the absence of PS, the observed decomposition products carbon disulfide and carbonyl sulfide are also plausible, as pure PBDS represents a hydrogen-poor environment, where phenols can form only if there are aromatic rings where carbon atoms undergo oxidation to provide the required hydrogen atoms.

Interaction Between PS and Radicals Originating in PBDS. Radicals originated by both PBDS decomposition pathways discussed above should also matter for an interaction with a PS matrix, the results of which are given in Figure 13.

It is predicted that abstraction of the tertiary C—H of PS by phenoxy radicals exhibits a ΔG close to zero (horizontal reaction pathway). In contrast to this, abstraction by aryl monothiyl and even more by aryl dithiyl radicals is significantly endergonic (vertical reaction pathways). However, for the monothiyl radical, the smallest H-abstraction barrier is computed, thus also this PS radical generation pathway can be expected to matter; altogether, all three H-abstraction events starting from the PBDS-derived radicals of Figure 13 require overcoming lower barriers than does radical generation out of pure PS (Figures 9–11). As soon as tertiary PS radicals have been formed, decomposition chemistry is possible with lower barriers than for these

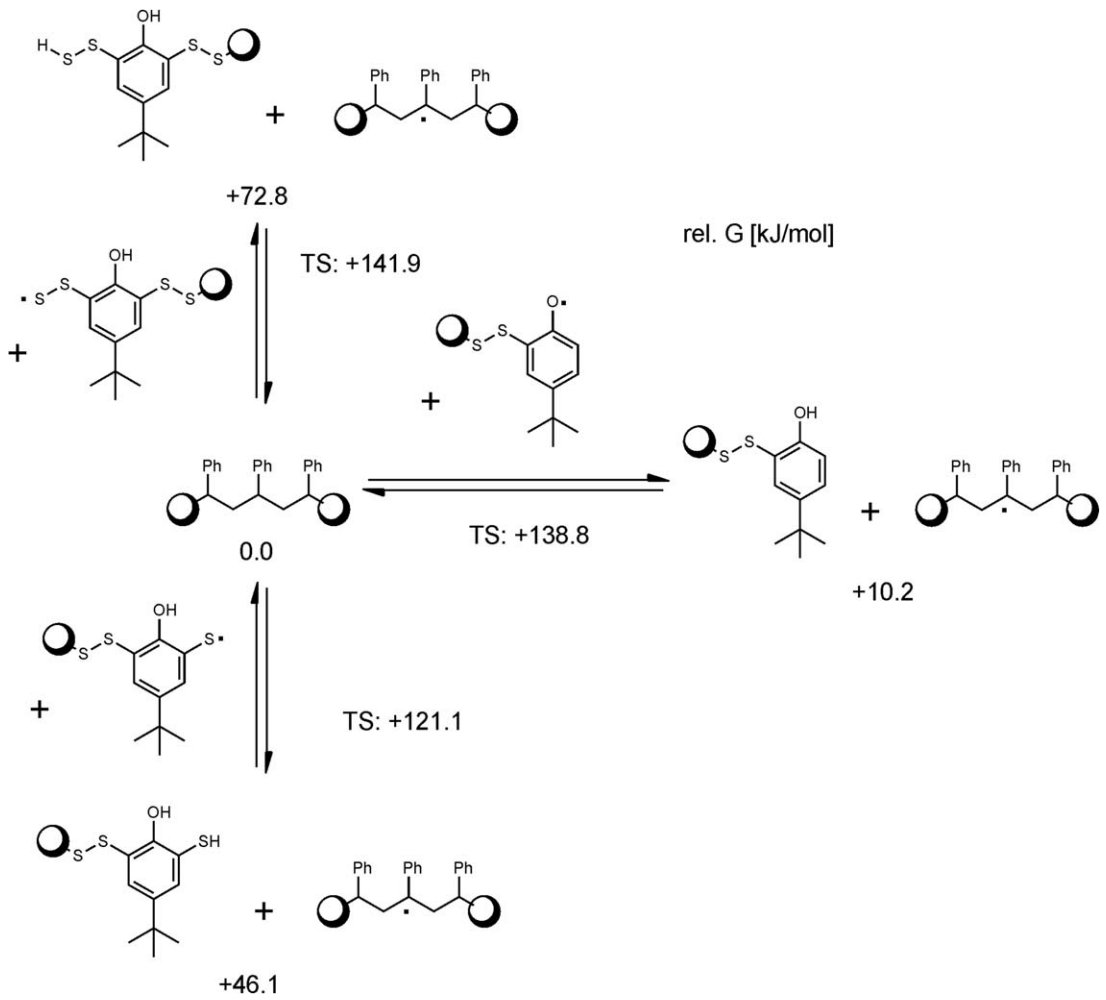

Figure 13. Computed relative Gibbs free energies for interaction of radical PBDS decomposition products with PS.

H-abstraction transition states (see below), and subsequent evaporation of volatile decomposition products makes these processes irreversible. However, it should also be kept in mind that the generated R-S-H or R-S-S-H species represent H-donors, and will also undergo reverse H-shift reactions (unless they evaporate), e.g., to secondary depolymerizing radicals, thus also contributing to a lower styrene formation close to the upper temperature limit.

Altogether, it can be concluded that PBDS is able to generate (initially mostly tertiary) PS radicals at a lower energetic cost than required for any C—C bond cleavage of the matrix itself. This means that PBDS yields higher radical concentrations in the PS matrix at temperatures where a pure PS would still be more or less free of radicals, which thus triggers decomposition at temperatures where PS itself would still be stable.

Radical Depolymerization of PS. In the above figures, various pathways have been proposed for the formation of secondary and tertiary PS radicals. As already suggested in Figures 9–11, the most probable fate of tertiary radicals is β-scission—leading to a double bond and a secondary radical—whereas secondary radicals depolymerize under styrene release. In addition to backbone cleavage, there is also intramolecular H-transfer, preferentially via six-membered rings ("backbiting" of secondary radicals), as an equilibration reaction between secondary and tertiary radicals. Computed results for these competing processes are given in Figure 14.

Compared with all C—C bond cleavages, backbiting is computed to exhibit a slightly lower barrier. Thus the equilibrium between secondary and the thermodynamically more stable tertiary radicals should establish itself quite fast. In this case, product selectivity of the decomposition is governed by the differences in Gibbs free energies of activation for β-scission leading to oligomers, and those of secondary radical decomposition to styrene.

In fact, decomposition starting from the tertiary radicals involves lower transition states and leads to more stable products. This is consistent with the higher amount of these oligomeric products observed upon low-temperature degradation in the case of adding PBDS. The very high styrene selectivity in the case of pure PS decomposition can be rationalized by the generally strong increase in rates with barriers of around 100 kJ mol^{-1} in the regime between 300°C and 400°C. For example, the rate coefficient of release of styrene from secondary radicals ($G^{+} = 101.4$ kJ mol^{-1}) increases from 6.9 $\times 10^{+3}$ s^{-1} to 1.9

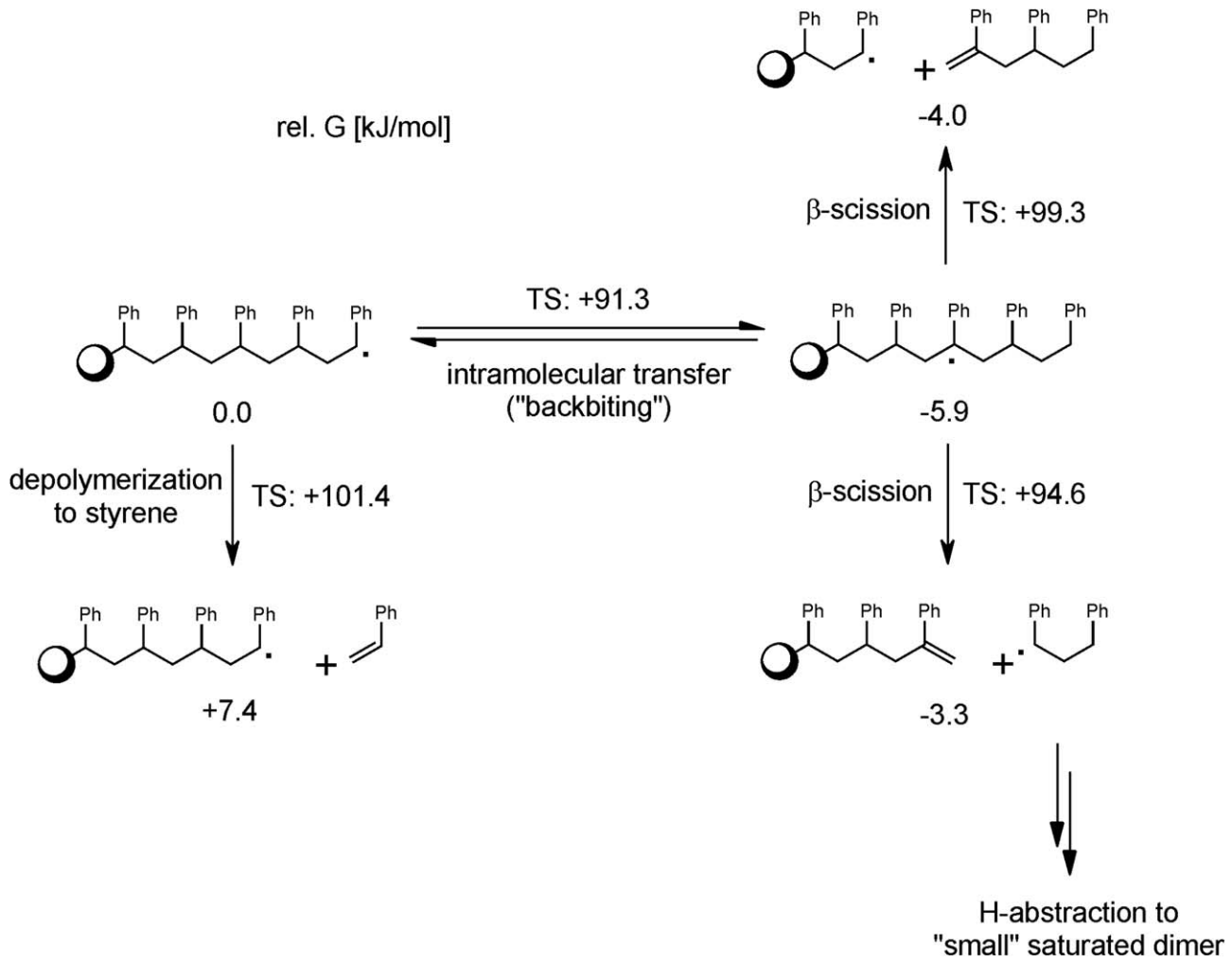

Figure 14. Computed relative Gibbs free energies for radical depolymerization of PS.

$\times 10^{+5}$ s^{-1}. Obviously, the higher the temperature, the less the equilibrating backbiting reaction is able to maintain the thermodynamic accessibility of the reaction channels towards oligomeric products, as the radical formed by all possible β-scissions of tertiary radicals is, again, a secondary one. On the molecular level, it appears in fact reasonable that depolymerization "triumphs" over backbiting with increasing temperature, as the former reaction means just dissociation of one C—C bond, which is entropically much less demanding than the formation of a specific cyclic transition state as required for backbiting.

CONCLUSION

In this article, we studied the thermal decomposition behavior of PS containing TPP and sulphur components: elemental sulphur and a phenolic disulphide. The investigations were performed by TGA-FTIR and solid-state FTIR investigations. Furthermore, a quantum chemical study of the interactions between PS and PBDS was performed.

We observed that there is an interaction of both additives and the polymer matrix in the condensed phase. TPP alone has no effect on the decomposition mechanism of PS. The sulphur components influence the decomposition of PS by reducing the mass release rate and the onset of decomposition temperature. This effect is only minor for elemental sulphur, but clearly detectable for the phenolic disulphide. For materials containing phenolic disulphide a decrease in styrene formation rate could be observed and an increase of oligostyrene formation. The investigation of various P : S ratios in PS as well as the decomposition behavior of binary mixtures revealed an interaction between the two additives. This interaction leads to an increased formation of radicalic sulphur species.

Some of these species can act via hydrogen abstraction even at lower temperatures, and, in so doing, influence the radical decomposition pathways such that the formation of styrene is suppressed in favour of oligostyrene.

In this work, we were able to show that radicalic decomposition processes of polymers can be influenced in the condensed phase by sulphur additives.

ACKNOWLEDGMENTS

The authors thank D. Neubert (BAM), F. Weber and A. Schnitzer (BASF SE) for the support in performing experiments.

REFERENCES

1. Beach, M. W.; Rondan, N. G.; Froese, R. D.; Gerhart, B. B.; Green, J. G.; Stobby, B. G.; Shmakov, A. G.; Shvartsberg, V. M.; Korobeinichev, O. P. *Polym. Degrad. Stab.* **2008**, *93*, 1664.
2. Weil, E. D.; Levchik, S. V. J. *Fire Sci.* **2007**, *25*, 241.
3. Hahn, K.; Fuchs, S.; Bellin, I.; Spies, P.; Hofmann, M.; Deglmann, P.; Massonne, K.; Denecke, H.; Fleckenstein, C.; Janssens, G.; Google Pat. **2011**, WO2011121001 A1.
4. Bellin, I.; Ciesielski, M.; Deglmann, P.; Denecke, H.; Döring, M.; Fleckenstein, C.; Fuchs, S.; Hahn, K.; Hofmann, M.; Janssens, G. Google Pat.: **2012**, WO2012089667 A1.
5. Cameron, G. G. *Die Makromol. Chem.* **1967**, *100*, 255.
6. Costa, L.; Camino, G.; Guyot, A.; Bert, M.; Chiotis, A. *Polym. Degrad. Stab.* **1982**, *4*, 245.
7. Costa, L.; Camino, G.; Guyot, A.; Bert, M.; Clouet, G.; Brossas, J. *Polym. Degrad. Stab.* **1986**, *14*, 85.
8. Kruse, T.; Sang Woo, O.; Broadbelt, L. *Chem. Eng. Sci.* **2001**, *56*, 971.
9. Li, J.; Wilkie, C. A. *Polym. Degrad. Stab.* **1997**, *57*, 293.
10. Wang, Z.; Jiang, D. D.; McKinney, M. A.; Wilkie, C. A. *Polym. Degrad. Stab.* **1999**, *64*, 387.
11. Levchik, G. F.; Si, K.; Levchik, S. V.; Camino, G.; Wilkie, C. A. *Polym. Degrad. Stab.* **1999**, *65*, 395.
12. Schnabel, W.; Levchik, G. F.; Wilkie, C. A.; Jiang, D. D.; Levchik, S. V. *Polym. Degrad. Stab.* **1999**, *63*, 365.
13. Miskolczi, N.; Bartha, L.; Deák, G. *Polym. Degrad. Stab.* **2006**, *91*, 517.
14. Serrano, D. P.; Aguado, J.; Escola, J. M. *Appl. Catal. B: Environ.* **2000**, *25*, 181.
15. Woo, O. S.; Ayala, N.; Broadbelt, L. J. *Catal. Today* **2000**, *55*, 161.
16. Bourbigot, S.; Gilman, J. W.; Wilkie, C. A. *Polym. Degrad. Stab.* **2004**, *84*, 483.
17. Jang, B. N.; Wilkie, C. A. *Polymer* **2005**, *46*, 2933.
18. Braun, U.; Schartel, B. *Macromol. Chem. Phys.* **2004**, *205*, 2185.
19. Braun, U.; Schartel, B. *Polym. Mater. Sci. Eng.* **2004**, *91*, 152.
20. Chang, S.; Xie, T.; Yang, G. *J. Appl. Polym. Sci.* **2008**, *110*, 2139.
21. Murashko, E. A.; Levchik, G. F.; Levchik, S. V.; Bright, D. A.; Dashevsky, S. *J. Fire Sci.* **1998**, *16*, 233.
22. Price, D.; Cunliffe, L. K.; Bullett, K. J.; Hull, T. R.; Milnes, G. J.; Ebdon, J. R.; Hunt, B. J.; Joseph, P. *Polym. Degrad. Stab.* **2007**, *92*, 1101.
23. Hirschler, M. M.; Thevaranjan, T. R. *Eur. Polym. J.* **1985**, *21*, 371.
24. Jakab, E.; Uddin, M. A.; Bhaskar, T.; Sakata, Y. *J. Anal. Appl. Pyrolysis* **2003**, *68–69*, 83.
25. Pawlowski, K. H.; Schartel, B. *Polym. Degrad. Stab.* **2008**, *93*, 657.
26. Eichkorn, K.; Treutler, O.; Öhm, H.; Häser, M.; Ahlrichs, R. *Chem. Phys. Lett.* **1995**, *242*, 652.
27. Vosko, S. H.; Wilk, L.; Nusair, M. *Can. J. Phys.* **1980**, *58*, 1200.
28. Perdew, J. P. *Phys. Rev. B* **1986**, *33*, 8822.
29. Schäfer, A.; Horn, H.; Ahlrichs, R. *J. Chem. Phys.* **1992**, *97*, 2571.
30. Klamt, A.; Schuurmann, G. *J. Chem. Soc. Perkin Trans.* **1993**, *2*, 799.
31. Zhao, Y.; Truhlar, D. *Theor. Chem. Account* **2008**, *120*, 215.
32. Dunning, T. H. *J. Chem. Phys.* **1989**, *90*, 1007.
33. Klamt, A.; Eckert, F. *Fluid Phase Equilibria* **2000**, *172*, 43.
34. Deglmann, P.; Müller, I.; Becker, F.; Schäfer, A.; Hungenberg, K.-D.; Weiß, H. *Macromol. Reaction Eng.* **2009**, *3*, n/a.
35. Schäfer, A.; Huber, C.; Ahlrichs, R. *J. Chem. Phys.* **1994**, *100*, 5829.
36. Ahlrichs, R.; Bär, M.; Häser, M.; Horn, H.; Kölmel, C. *Chem. Phys. Lett.* **1989**, *162*, 165.
37. Bylaska, E. J.; de Jong, W. A.; Govind, N.; Kowalski, K.; Straatsma, T. P.; Valiev, M.; Wang, D.; Apra, E.; Windus, T. L.; Hammond, J.; Nichols, P.; Hirata, S.; Hackler, M. T.; Zhao, Y.; Fan, P. D.; Harrison, R. J.; Dupuis, M.; Smith, D. M. A.; Nieplocha, J.; Tipparaju, V.; Krishnan, M.; Vazquez-Mayagoitia, A.; Wu, Q.; Van Voorhis, T.; Auer, A. A.; Nooijen, M.; Crosby, L. D.; Brown, E.; Cisneros, G.; Fann, G. I.; Fruchtl, H.; Garza, J.; Hirao, K.; Kendall, R.; Nichols, J. A.; Tsemekhman, K.; Wolinski, K.; Anchell, J.; Bernholdt, D.; Borowski, P.; Clark, T.; Clerc, D.; Dachsel, H.; Deegan, M.; Dyall, K.; Elwood, D.; Glendening, E.; Gutowski, M.; Hess, A.; Jaffe, J.; Johnson, B.; Ju, J.; Kobayashi, R.; Kutteh, R.; Lin, Z.; Littlefield, R.; Long, X.; Meng, B.; Nakajima, T.; Niu, S.; Pollack, L.; Rosing, M.; Sandrone, G.; Stave, M.; Taylor, H.; Thomas, G.; van Lenthe, J.; Wong, A.; Zhang, Z. Pacific Northwest National Laboratory Richland, Washington, US, **2009**.
38. Zweifel, H.; Maier, R. D.; Schiller, M. Plastic additve handbook; Carl Hanser Verlag: Munich Germany, **2009**.
39. Montaudo, G.; Puglisi, C.; Blazò, M.; Kishore, K.; Ganesh, K. *J. Anal. Appl. Pyrolysis* **1994**, *29*, 207.